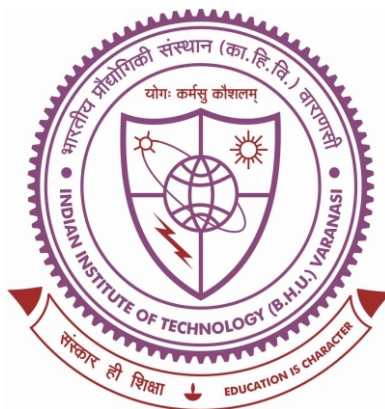


Nanoscale charge heterogeneity and chaotic resistive switching in VO₂-based Mott memristors



Thesis submitted in the partial fulfillment for the
Award of Degree

Doctor of Philosophy

By

Pawan Kumar Ojha

SCHOOL OF MATERIALS SCIENCE & TECHNOLOGY
INDIAN INSTITUTE OF TECHNOLOGY
(BANARAS HINDU UNIVERSITY)
VARANASI - 221005
INDIA

Roll No. 18111503

2024

Dedicated to
My Beloved Family

CERTIFICATE

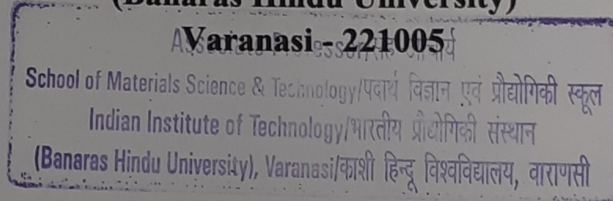
It is certified that the work contained in the thesis titled "*Nanoscale charge heterogeneity and chaotic resistive switching in VO₂-based Mott memristors*" by "*Mr. Pawan Kumar Ojha*" has been carried out under my supervision and that this work has not been submitted elsewhere for a degree.

It is further certified that the student has fulfilled all the requirements of Comprehensive, Candidacy, and SOTA for the award of Ph.D. Degree.

SK Mishra
09/09/2024

Dr. Shrawan Kumar Mishra
(Supervisor)

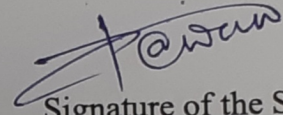
School of Materials Science & Technology
Indian Institute of Technology
(Banaras Hindu University)



DECLARATION BY THE CANDIDATE

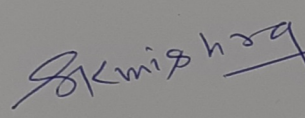
I, "**Pawan Kumar Ojha**", certify that the work embodied in this thesis is my own bona fide work and carried out by me under the supervision of "**Dr. Shrawan Kumar Mishra**" from "**January 2019**" to "**April 2024**", at the "**School of Materials Science & Technology**", Indian Institute of Technology (Banaras Hindu University), Varanasi. The matter embodied in this thesis has not been submitted for the award of any other degree/diploma. I declare that I have faithfully acknowledged and given credits to the research workers wherever their works have been cited in my work in this thesis. I further declare that I have not willfully copied any other's work, paragraphs, text, data, results, etc., reported in journals, books, magazines, reports, dissertations, thesis, etc., or available at websites and have not included them in this thesis and have not cited as my own work.

Date: 09/09/2024
Place: Varanasi


Signature of the Student
(**Pawan Kumar Ojha**)

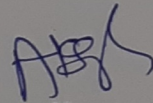
CERTIFICATE BY THE SUPERVISOR

It is certified that the above statement made by the student is correct to the best of my knowledge.


09/09/2024

Dr. Shrawan Kumar Mishra
School of Materials Science & Technology
IIT (BHU), Varanasi

Associate Professor
School of Materials Science & Technology/पदार्थ विज्ञान एवं प्रौद्योगिकी स्कूल
Indian Institute of Technology/भारतीय प्रौद्योगिकी संस्थान
(Banaras Hindu University), Varanasi/काशी हिन्दू विश्वविद्यालय, वाराणसी


Coordinator

School of Materials Science & Technology

IIT (BHU), Varanasi
School of Materials Science & Technology/पदार्थ विज्ञान एवं प्रौद्योगिकी स्कूल
Indian Institute of Technology/भारतीय प्रौद्योगिकी संस्थान
(Banaras Hindu University), Varanasi/काशी हिन्दू विश्वविद्यालय, वाराणसी

COPYRIGHT TRANSFER CERTIFICATE

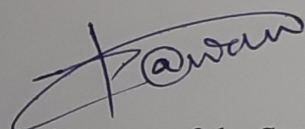
Title of the Thesis: **Nanoscale charge heterogeneity and chaotic resistive switching in VO₂-based Mott memristors**

Name of the Student: **Pawan Kumar Ojha**

Copyright Transfer

The undersigned hereby assigns to the Indian Institute of Technology (Banaras Hindu University) Varanasi all rights under copyright that may exist in and for the above thesis submitted for the award of the "*Doctor of Philosophy*" degree.

Date: 09/09/2024
Place: Varanasi



Signature of the Student
(**Pawan Kumar Ojha**)

Note: However, the author may reproduce or authorize others to reproduce material extracted verbatim from the thesis or derivative of the thesis for author's personal use provided that the source and the Institute's copyright notice are indicated.

Acknowledgements

A research project like this is never the work of anyone alone. The contributions of many different people, in their different ways, have made this possible. I would like to extend my gratitude to the many people who helped to bring this research project to completion. This journey would not have been possible without the support of my family, professors, mentors, and friends.

*My first and foremost heartfelt gratitude and indebtedness would be towards Bharat Ratna **Mahamana Pandit Madan Mohan Malviya Ji**, the founder of Banaras Hindu University, who sacrificed his entire life and efforts in establishing this artistic temple of knowledge and wisdom.*

*I would like to express my sincere gratitude to my supervisor, **Dr. Shrawan Kumar Mishra**, Associate Professor, School of Materials Science & Technology, Indian Institute of Technology (Banaras Hindu University), Varanasi for providing me the opportunity to work in his research group. I am so deeply grateful for his help, professionalism, valuable guidance, everlasting enthusiasm and unstained support throughout my Ph.D. His deep insights helped me at various stages of my research. Finally, I am extremely thankful to him for the freedom he gave me during the course of my research work.*

*I cannot find words to express my gratitude to my pedagogue, **Prof. Shankar Ram**, Retired Professor, Materials Science Centre, IIT Kharagpur. His critical remarks and suggestions have always been very helpful in improving my skills.*

I would also like to express my sincere thanks to RPEC members Dr. Bhola Nath Pal, School of Materials Science & Technology, IIT (BHU), and Dr. Swapnil Patil, Department of Physics, IIT (BHU), for their fascinating advice and criticism, which encouraged me to broaden my research from numerous viewpoints. I would like to thank the coordinator of the School of Materials Science and Technology, IIT (BHU) for providing different instrumental facilities. I would like to express my sincere gratitude to Dr. Nikhil Kumar (DPGC convener) for his valuable inputs, suggestions and affectionate mannerism.

I would also like to acknowledge fruitful support and guidance of all the teacher of the school Prof. D. Pandey, Prof. R. Prakash, Prof. P. Maiti, Dr. (Mrs.) C. Rath, Dr. A. K. Singh, Dr. C. Upadhyay, Dr. B. N. Pal, Dr. S. Singh, Dr. A. K. Mishra, Dr. N. Kumar, Dr. R. Panwar and Dr. A. Kumar for their kind support at all moment during the progress of my research.

I would like to convey my heartfelt gratitude to CIFC, IIT (BHU), Varanasi, Dr. Vasant G. Sathe, UGC-DAE Consortium for Scientific Research, Indore and Dr. Deepash Shekhar Saini, Department of Physics, DDU Gorakhpur University, Gorakhpur and Dr. Bogdan Sava, Engineer at neaspec (attocube systems AG) for their assistance in carrying out the characterization of the synthesized samples. I'm also grateful to the school's staff members and the IIT (BHU) officials for their assistance in completing my thesis during my stay.

With a special thanks to my seniors, lab mates and cheerful group of colleagues Dr. Shyam Babu, Ms. Rajnandini Sharma, Ms. Nitipriya Tripathi, Ms. Simran Sahoo, Mr. Arkaprava Mondal, Mr. D. Rakesh, Mr. Eeshan Ketkar and rest of the energetic youngest group members for their suggestion and healthy discussion of my research issues. I am extremely thankful to my friends Mrs. Kavita Choudhary, Dr. Vishwas Acharya, Mr. Vishal Srivastava, Dr. Rajnikant Upadhyay, Mr. Ashish Kumar Choksey, Mr. Deepak Rathore, Mr. Jaynarayan Mishra, Mr. Taranga Dehury, Mr. Rohit Rodhia, Mr. Shivam Choubey, Mr. Prosun Mondal, Dr. Ravi Patel, Ms. Urvashi Kesarwani, Mrs. Divya Pareek, Dr. Priya Singh, Dr. Ankita Singh and Mr. Prince Mourya for their support, cooperation and sincere help in many ways as well as for making my stay here enjoyable and for their time-to-time encouragement during my bad situations. I would like to thank Department of Science and Technology (DST), New Delhi for financial assistance (Senior Research Fellowship).

*I am especially grateful to my parents, **Mr. Ramdev Ojha** and **Mrs. Sharda Ojha** who supported me emotionally and financially. I always knew that you believed in me and wanted the best for me. Thank you for teaching me that my job in life was to learn, to be happy, to know and understand myself; only then could I know and understand others. I must express my very profound gratitude to my sister Mrs. Rajshree Ojha, Mrs. Kavita Ojha, Ms. Usha Ojha and my brother, C. A. Krishan Kumar Ojha and my nephew Mr. Harshwardhan Saraswat for providing me with unfailing support and continuous*

encouragement throughout my years of study and through the process of researching and writing this thesis. Thank God for the wisdom and perseverance that he has bestowed upon me during this research project and indeed throughout my life to give such a wonderful opportunity and given me the strength to accomplish the assignment.

~ Pawan Kumar Ojha

LIST OF FIGURES

Figure 1.1 Schematic parameters associated during heating cooling thermal cycles.....	4
Figure 1.2 SMT and Néel temperatures in Magneli families.	6
Figure 1.3 VO ₂ phases and their conditions of transformation.....	7
Figure 1.4 Crystal representations of (a) VO ₂ (M) and (b) VO ₂ (R). Perspectives along the c _R -axis of monoclinic (twisted V-V dimers) (c) and tetragonal (d) structures, respectively.	10
Figure 1.5 Atomic structure of VO ₂ M ₁ , M ₂ and R phase.....	11
Figure 1.6 Band structure of VO ₂ as described by Goodenough.	12
Figure 1.7 Phase diagram illustrating the impact of temperature stress on single crystals of VO ₂	14
Figure 1.8 The octahedral arrangement of the V cation in various V _x O _y , phases, and the effect of coupling between the competing spin, charge, and orbital degrees of freedom on the optical and electronic properties in VO ₂	16
Figure 1.9 Diagram illustrating the schematic energy band structure of VO ₂	17
Figure 1.10 Depiction of VO ₂ utilization in various field.	21
Figure 1.11 (A) Fundamental theoretical circuit components, and (B) pinched hysteresis I-V loop of the memristor.	24
Figure 2.1 The experimental steps (schematics) used to reduce V ₂ O ₅ → 2VO ₂ + ½O ₂ ↑ in an aqueous acid followed by adding a polymer PVP to form a hydrogel suitable to spin coating (after heating at 353 K in the air) on pure and SiO ₂ /TiO ₂ coated Si(p ⁺⁺).	42
Figure 2.2 The cleaning and fabrication steps (schematics) used to deposit VO ₂ thin film form a hydrogel suitable through spin coating on pure and SiO ₂ /TiO ₂ coated Si(p ⁺⁺) (Bottom panel shows the final device structure of TFMs).	45
Figure 2.3 A graphical representation of Bragg's law equation.	48
Figure 2.4 Schematic diagram of a typical AFM setup.	49
Figure 2.5 Schematic diagram of FESEM.	51
Figure 2.6 Schematic diagram of a dispersive Raman spectrometer setup.	53

Figure 2.7 Diagram illustrating the setup of a s-SNOM imaging system functioning in a pseudo-heterodyne configuration and bottom image shows a close view of a tiny aperture illumination.56

Figure 2.8 Circuit configuration for a four-point probe conducting impedance measurements.57

Figure 3.1 (a) The XRD spectra of VO₂ thin film. The Bragg's peak across 27.29° and 57.11° correspond to the (011) and (022) peaks of the monoclinic (M₁) phase. (b) the highlighted part of (011) Bragg's peak along with its pseudo-Voigt function fit. Both experimental and simulation data are well-matched. An accurate value of the D_e is estimated.68

Figure 3.2 VO₂ NCs were imaged through a TEM at a nano-length scale by dispersing crystallites on top of a carbon-coated mesh. (d) Illustrates the well-ordered lattice fringes in (011) crystallographic direction, imaged by employing HR-TEM.69

Figure 3.3 (a) I-V characteristics of the VO₂/SiO₂(Si) measured in vertical geometry between 0-5 V at RT. The electric-field-triggered SMT is observed at RT. (b) PF plot of the I-V curves log(I/V) vs √V. Three regions metallic, Ohmic and PF dominating are defined. The dotted green lines in the PF region are for visual guidance, indicating the dominating of the PF conduction mechanism in that region.70

Figure 3.4 Raman modes measured for representative VO₂ thin film as a function of temperature during (a) Heating and (b) cooling cycles. The Raman frequencies ν₁ and ν₂ show the FWHM and intensity vary as a function of temperature, suggesting a robust structural link, (c) variation of Raman frequencies ν₁ and ν₂ during heating/cooling cycles, (d) evidence of hole burning in Raman spectra during a heating and cooling cycle.72

Figure 3.5 (a) The temperature-dependent sheet resistance of representative VO₂ thin film. The change in resistance suggests three different regions: SC, mixed-phase and metallic phase. (b) The variation of FWHM of V-V dimers (b) (191.93 cm⁻¹) and (c) V-O bond (222.5 cm⁻¹) frequencies as a function of temperature across the SMT during heating/cooling cycles. (d) Resistance vs puddles size plot, which is simulated for both heating and cooling. For each thermal cycle, critical temperatures, T_{C1} and T_{C2}, are shown. Dashed vertical lines indicate T_{C1} and T_{C2} calculated from EMA during heating/cooling cycles. (e) The scattering cross section as a function of puddles size is well corroborated with resistance vs puddles size plot.75

Figure 4.1 (a → d) FESEM images of SiO ₂ and TiO ₂ thin films on a Si(<i>p</i> ⁺⁺) substrate. Small SiO ₂ /TiO ₂ clusters are visible in magnified (b, d) FESEM images.	84
Figure 4.2 AFM images of VO ₂ films grown on a Si(<i>p</i> ⁺⁺) substrate (a) before and after using a buffer layer (b) SiO ₂ and (c) TiO ₂ . A 3D image (at bottom) shows (c) a smooth surface (1.8 nm rms).	85
Figure 4.3 XRD patterns of the VO ₂ films grown on (a) TiO ₂ , (b) SiO ₂ and (c) Si.	87
Figure 4.4 FESEM images of the VO ₂ films grown on (a) Si, (b) SiO ₂ and (c) TiO ₂	89
Figure 4.5 The XPS bands O1s _{1/2} and V2p _{1/2,3/2} in thin films VO ₂ grown at (a, b) bare and (c, d) TiO ₂ coated Si, respectively.	90
Figure 4.6 (a) Schematics of an AM and a BBAM, (b) a typical VO ₂ @TiO ₂ -Si memristor, and I-V plots for the films VO ₂ grown at (100) Si (c) before and after a nano-gate (d) SiO ₂ and TiO ₂ , and (f) power outputs regulated at the films at different fields.	96
Figure 4.7 Modulated (a, b, c) resistance (ρ_e) and (d) reciprocal of current (I_e^{-1}) measured at an increasing voltage (towards arrows) for thin VO ₂ films grown at (a) Si, (b) SiO ₂ and (c) TiO ₂	97
Figure 5.1 (a) XRD pattern of (011) uniaxial M ₁ -VO ₂ grown at Si (<i>p</i> ⁺⁺) via a SiO ₂ nanogate (of XRD in the inset). The (011) peak zoomed in the inset shows its symmetric shape. *The SiO ₂ peak. (b) A compressive d ₀₂₂ strain, (c) an R-VO ₂ lattice order at a coherent (011) M ₁ -VO ₂ facet along the film, (d) a strain induced R ↔ M ₁ -VO ₂ order, (e) a charge-induced VO ₂ bonding @SiO ₂ /Si surface, and (f) an M ₁ -VO ₂ surface order (on heating) leading to the SC → metallic VO ₂ states at 3d ¹ -V ⁴⁺ delocalized electrons at the planar 2D nanostrips.	106
Figure 5.2 HRTEM images of (a) distorted polytopes and (b) thin layers (plates), (c) SAED pattern (plate A) of d ₀₁₁ = d ₀₁₁ ≅ 0.3250 nm, d ₀₂₂ ≅ 0.1620 nm and d ₀₃₃ ≅ 0.1050 nm arrays of spots superposed on diffused rings of radii r ₀₁₁ = (0.3730 nm) ⁻¹ , r ₀₂₂ = (0.1860 nm) ⁻¹ and r ₀₃₃ = (0.1210 nm) ⁻¹ of a disorder VO ₂ , (d, e, f) lattices from different parts at plate A, (g) a model two-phase structure, and (h, i) 2D/3D AFM images from the VO ₂ @SiO ₂ -Si films. Twins in (c) are marked at the circles.	108
Figure 5.3 The near-field MIR s-SNOM images at surface phase order in a thin M ₁ -VO ₂ film at 303 K → 343 K (panels 1, 2), with a closer view of thermal contrast across the T _c	

in panel-3. At the bottom, a model projects a competing $M_1 \rightarrow M_2 \rightarrow R_1 \rightarrow R_2/R\text{-VO}_2$ order. 111

Figure 5.4 (a) The σ_{ac} as a function of frequency (1 Hz to 10^6 Hz) at the thin film $\text{VO}_2@SiO_2\text{-Si}$ at 303 K to 353 K across the T_c point, (b) temperature dependent σ_{ac} and (c) its derivatives at selected frequencies showing thermal induced $M_1 \rightarrow M_2/R_1/R_2/R\text{-VO}_2$ orders, and (d, e) model band-energy diagrams at thermal/frequency induced charge orders. 114

Figure 5.5 The real Z' (a) and imaginary Z'' (b) parts of impedance resistance, which are zoomed in (c, d) respectively, showing frequency-induced partial $M_1 \rightarrow M_2 \rightarrow R_1/R_2/R\text{-VO}_2$ orders at the films $\text{VO}_2@SiO_2\text{-Si}$ at temperature is raised in steps of 10 K over 303 K to 393 K. (e, f) Decreased Z' and Z'' at dominant $R_1, R_2, R\text{-VO}_2$ states. 116

Figure 5.6 Nyquist plots at frequency (10^2 Hz to 10^6 Hz) induced charge order in a film $\text{VO}_2@SiO_2\text{-Si}$ at (a) 303 K to 353 K and (b) 363 K to 473 K (taken at 10 K intervals), (c) with Z'' derivatives (Z''^*) (a) plots over Z' showing the itinerant transitions. The insets present (a) a LCR circuit at an inductance L (resistance R_x) and an external resistance R' , and a closer view $Z''\text{-}Z'$ at (a, b) the intermediate VO_2 states. (d) A model phase diagram of itinerant VO_2 states over the temperatures/frequencies. 118

Figure 5.7 Thermal response of (a) R_o , (b) L and (c) C_p in an equivalent LCR circuit at a film $\text{VO}_2@SiO_2\text{-Si}$, showing the $T_c \sim 353$ K (vertical line). While the R_o and L are rapidly diminished, the C_p is rapidly enhanced at the T_c point, and arises up linearly at deep metallic $R\text{-VO}_2$ states. (d) A closer R_o view of it rises up gradually at a nonlinear α_R over T^{-1} , with weak inflections at 415 K and 450 K, and (e) a model $M_1 \rightarrow M_2/R_1/R_2\text{-}R\text{-VO}_2$ order at frequencies (RT). 120

Figure 5.8 A model distribution of a thermal-induced charge-density ρ_e orders as a function temperature in a correlated (a) $M_1 \rightarrow M_2\text{-VO}_2$ and (b) $R_2 \rightarrow R\text{-VO}_2$ phase order. The powers η and ϑ are regularly declined 5.0 to 1.5 at (a) $\gamma_1 = 2.5 \times 10^{-3} \text{ K}^{-\eta}$ and (b) $\gamma_2 = 2.5 \times 10^{-3} \text{ K}^{-\eta}$ in the model relations (7) and (8), respectively. The plots made at varied modulators γ_1/γ_2 over $0.5 \times 10^{-3} \text{ K}^{-\eta}$ to $3.0 \times 10^{-3} \text{ K}^{-\eta}$ at $\eta = 5.0$ and $\vartheta = 2.5$ are added in the insets, respectively. 123

LIST OF TABLES

Table 1.1 Physical parameter of VO ₂ at monoclinic and rutile crystal structure.	9
Table 2.1 The different techniques for VO ₂ thin film deposition.	38
Table 4.1 The XRD peaks in the effects of a SiO ₂ /TiO ₂ gate regulates a uniaxial (011) VO ₂ bonding on a (100) Si(<i>p</i> ⁺⁺) substrate in thin films.	86
Table 4.2 The XPS bands in the effects of a n-TiO ₂ gate regulates (011) VO ₂ bonding on a (100) Si(<i>p</i> ⁺⁺) substrate in thin films.	92
Table 4.3 The effects of a nano SiO ₂ /TiO ₂ gate on energy stored in the hysteresis I-V loops in the VO ₂ films grown at a Si(<i>p</i> ⁺⁺) substrate.	94

LIST OF ABBREVIATIONS

VO₂	Vanadium Dioxide
SC	Semiconductor
SMT	Semiconductor → Metal Transition
DFT	Density Functional Theory
VOs	Vanadium Oxides
IR	Infrared
UV	Ultraviolet
MST	Metal → Semiconductor Transition
PF	Poole Frenkel
XRD	X-ray Diffraction
FWHM	Full Width at Half Maximum
NCs	Nanocrystals
NAs	Nano-architects
PLD	Pulse Laser Deposition
ALD	Atomic Layer Deposition
PVP	Poly(vinyl pyrrolidone)
TFMs	Thin Film Memristors
AFM	Atomic Force Microscopy
FESEM	Field-Emission Scanning Electron Microscopy
s-SNOM	Scattering-Type Scanning Near-Field Optical Microscopy
BBAM	Bistable Bi-Local Active Memristor
AM	Active Memristor
SEDs	Single Electric Domains

HRTEM	High-Resolution Transmission Electron Microscopy
SAED	Selected Area Electron Diffraction
VC	Valance Band
CB	Conduction Band
RFs	Radio Frequencies
MIR	Mid-infrared

LIST OF SYMBOLS

T_N	Néel Temperature
T_c	Critical Temperature
$e-p$	Electron-Phonon
V_{th}	Threshold Voltage
D_e	Crystallite Size
2θ	Diffraction Angle
D	Dimension
V_t	Threshold Field
ρ_e	Effective Resistance
E_l	Anisotropic Electric Field
Z	Impedance Resistance
σ_{ac}	Conductivity
γ_c	Compressive Strain
V_c	Lattice Volume
E_F	Fermi Level
E_g	Bandgap
α_R	Thermal Coefficient
E_b	Binding Energy
I_p	Intensities

ABSTRACT

Vanadium dioxide (VO_2) - a non-stoichiometric oxide semiconductor (SC) offers exotic properties at a self-confined structure of correlated $3d^1$ -electrons (spins) useful for non-volatile memory devices, smart switches, and human brain-inspired neuromorphic devices due to correlated phase/charge orders of SC to metallic states. Poor chemical stability and fragile nature limit its technologies of thin films. In view of resolving some of these issues, we developed polymer stabilized VO_2 films (thickness $t \leq 100$ nm), using VO_2 nanocolloids in poly(vinylpyrrolidone) (PVP) (as a VO_2 dispersoid, a molecular template, and a film former) in water, at a (100) $\text{Si}(p^{++})$ substrate. Using a nano $\text{SiO}_2/\text{TiO}_2$ gate ($t \leq 10$ nm), VO_2 is grown (011) preferentially in a confined shape of nanoplates (nanocrystals) along the films, mostly of 15 to 40 nm widths at 20–30 nm crystallite size. The results are described with X-ray diffraction (XRD), surface topologies, lattice images, and X-ray photoelectron spectroscopy (XPS) of films in the variable charges order at the itinerant metallic states. A significant $\text{V}^{5+}\text{-}3d^0$, ≤ 33 at%, is shown in the XPS bands, which induces metallic states at conducting ' $\text{V}^{4+} \rightarrow \text{V}^{5+} + e^-$ ' channels. So, a charge-regulated SC \rightarrow metal transition incurs via an induced $\text{M}_1 \rightarrow \text{R-VO}_2$ metallic state near room temperature.

Employing temperature-controlled Raman spectroscopy, we demonstrate V-V dimers softening in nanostructured VO_2 thin films. Temperature-dependent Raman band shifts and their spectral width (FWHM) suggest an intriguing phonon characteristic that evolves across the semiconductor \rightarrow metal transition (SMT) during the heating/cooling thermal cycles. The V-V dimers start to collapse above a critical temperature ($T_c > T_{\text{MIT}}$) and restoring their initial phase during the cooling process below T_{MIT} . Raman bands suggest an abrupt reversible switching in the optical behaviour at a temperature ($T_o = 332$ K).

Temperature-dependent sheet resistance variations indicate a smooth reversible resistive switching relatively at a lower temperature ($T_e = 340$ K). The difference in transition temperatures has been discussed in the framework of light scattering cross-section from the metallic domains that become more extensive at the critical length scale required for percolation conduction in resistive switching. 2D-mean-field approximation associated with Mie scattering are modelled to explain the percolation process during phase transition and to estimate the metallic domain length scale evolved in the semiconducting matrix across the SMT. Our experimental findings explain the occurrence of optical and electrical transitions at the distinct temperature range, suggesting a weak coupling between lattice and optical switching.

A memristor $\text{VO}_2/\text{TiO}_2/\text{Si}$ renders a wide current-voltage (I-V) loop at room temperature, with a leakage current that is well controlled at a high-k TiO_2 gate. It exhibits a reversible switching at a duly small threshold field, $V_t \leq 0.2$ V. This is the smallest V_t tuned reported so far, which is beneficial for the low field, ≤ 1.0 V, devices. The charge models corroborate the effect of field-induced charge order at the interfaces of ‘conducting through channels’, regulating a reversible I-V hysteresis in an ON/OFF cycle. Thin VO_2 films of unified (011) nanocrystals (NCs) readily metallize at surface charge order on the vibrant NCs (as mini capacitors) in a pool. At the NCs, a nanoscale phase VO_2 can order in a confined domain of temperature (or other stimulus) in a first-order surface phase order, without a phase separation. At a critical charge density, $3d^1\text{-V}^{4+}$ electrons (e) decouple from the phonons (p) and order in delocalized VO_2 states. Accordingly, it is shown that as the frequency (stimuli) is raised 10^2 to 10^6 Hz, the impedance resistance in thin films $\text{VO}_2/\text{SiO}_2/\text{Si}$ is declined (up to 10^5 times at the room temperature), leading to successive $M_1 \rightarrow M_2/R_1/R_2/R\text{-VO}_2$ phase orders over the $M_1\text{-VO}_2$ resistive states. The frequency induces, regulates, and monitors exotic charges of

drive the phase order. A metallic R-VO₂ phase thus orders even at 303 K (at 10⁵ Hz) that gradually shifts at higher frequencies (up to 10⁶ Hz) upon heating to 343 K, i.e. the T_c point at zero frequency. The distinct VO₂ phases are well mapped in the s-SNOM (scattering-type scanning near-field optical microscopy) images at mid-infrared (MIR) bands. A density functional theory is applied to model the phase order at successively decoupled 'e-p' states. The results insight the mechanisms of 3d¹-V⁴⁺ electrons decouple and order leading to the metallic VO₂ states.

PREFACE

The swift progression of modern technology necessitates a constant enhancement of electronic device performance. Achieving this improvement requires a comprehensive understanding of the fundamental behavior of materials used in technology. In the post-Moore era, newly introduced materials defy classical solid-state physics theories, displaying unconventional properties that can be harnessed for the development of advanced electronic devices. Transition metal oxides are captivating due to their diverse range of properties, exhibiting both metallic and semiconducting behaviours, along with superconductivity featuring remarkably high critical temperatures. The intricate physical behavior of these compounds arises primarily from the distinctive environment housing electric charges. The chemical bonds between the d-orbitals of multivalent transition metals and the p-orbitals of highly electronegative oxygen anions give rise to energy bands characterized by narrow widths and strong directionality. Consequently, there is a robust coupling between charge, spin, and orbital degrees of freedom. These compounds showcase various electronic configurations, significant electron-electron and electron-phonon interactions, as well as confined electronic systems. The development of thin films of transition metal oxides on a single crystal substrate provides the opportunity to customize material properties by specifying factors such as crystal structure, direction, uniaxial strain, chemical composition, and film thickness. The sol-gel technique proves to be a fitting method for producing crystalline oxide thin films in this context.

The distinctive characteristics of VO_2 position it as one of the most captivating transition metal oxides. VO_2 is a correlated material that undergoes a SMT in the vicinity of room RT. This transition is influenced by the robust correlation among electrons in the d-orbital

of vanadium and is concomitant with a significant structural modification that substantially alters the energy band diagram of the material.

The intricate examination of this transition has been a focal point for numerous researchers over the past fifty years, and it continues to be an unresolved inquiry. The SMT has also been triggered through the application of an electric field in a transistor like device, employing either an oxide layer or an electrolyte as a gate. One explanation for the electric-field-induced transition posits that a Mott transition occurs at the surface of the thin film of VO₂, extending throughout the entire film thickness. This implies that the behavior is highly contingent on the substrate on which the VO₂ thin film is grown, as the film properties and its response to an applied electric field vary based on the substrate's crystal structure and orientation. Clarifying the specific phenomena accountable for the electric-field-induced transition is crucial for a comprehensive understanding.

Simultaneously, we examined the characteristics of VO₂ thin films cultivated on three distinct substrates: Si (100), SiO₂ (100), and anatase TiO₂. These thin films were employed in the creation of memristor devices designed to operate at RT. A comparison of the performance of these devices with those fabricated on various substrates provides valuable insights into the behavior of VO₂ during the SMT.

The thesis is structured into several chapters, each of which is outlined below.

Chapter 1, deals with an introduction to the thesis, delving into the motivation and rationale for selecting vanadium dioxide as a Mott type SC. The chapter explores the theoretical background that underlies the investigation of SMT, emphasizing the unique properties of VO₂ in this context. Additionally, this chapter outlines the potential applications of VO₂ in next-generation memory devices, shedding light on the relevance and significance of studying its behavior during SMT. This comprehensive overview sets

the stage for the subsequent chapters, providing a clear foundation for understanding the research objectives and contributions presented in the thesis.

Chapter 2, presents an intricate exploration of the synthesis methodology (growth processes of VO₂ thin films and SiO₂/TiO₂ nanogate) focusing on the sol-gel based spin coating technique and the subsequent fabrication of devices. The chapter not only outlines the step-by-step process involved in these procedures but also elucidates the underlying working principles. Furthermore, a comprehensive overview is provided for the experimental setup for various characterization methods employed in the present thesis including XRD, TEM, FESEM, AFM, XPS, Raman Spectroscopy, four-probe measurements, semiconductor device analyzer, Impedance Spectroscopy, and s-SNOM.

Chapter 3, offers an in-depth examination is conducted on the temperature-induced phase transition within a nanostructured VO₂ thin film. The chapter provides into the intricacies of the optical phase transition, leveraging insights derived from Raman spectroscopy data.

A key focus is the exploration of variable sizes for charge puddles within the VO₂ samples, providing a comprehensive understanding of their distribution between different phases. This investigation sheds light on the universality of charge puddles in VO₂ samples during the phase transition, offering valuable insights into the nuanced behavior of the material under varying temperature conditions. The detailed analysis and findings presented in this chapter contribute significantly to unravelling the complexities of the temperature-induced phase transition in nanostructured VO₂ thin film.

Chapter 4, presents a comprehensive analysis is provided on the development of prototype low-field memristor devices, constructed from VO₂ films. The chapter delves into the intricacies of the role played by a nanogate composed of SiO₂/TiO₂ in facilitating

charge transfer within the VO₂@(100) Si(p⁺⁺) films. Specifically, the investigation focuses on the impact of a low-field 0 ↔ 5 V swipe on the device's performance.

The experimental results reveal noteworthy outcomes, notably achieving a remarkably small threshold voltage of V_t = 0.12 V during the low-field operation. These findings underscore the effectiveness and significance of the SiO₂/TiO₂ nanogate structures in modulating charge transfer within the VO₂ thin films, particularly in the context of low-field applications.

Chapter 5, systematically investigates a series of M₁ → M₂/R₁/R₂/R-VO₂ phases in detail. The s-SNOM images of VO₂ films effectively map all five VO₂ phases in the mid-infrared (MIR) field. These findings suggest a kinetic response of the critical temperature (T_c) point influenced by the decoupled 3d¹ electrons (orbitals). Consequently, the T_c point consistently shifts from 343 K under terahertz (THz) (5-10 meV) conditions to 353 K under MIR (125 meV) fields employed in the s-SNOM imaging at the nanoscale.

Chapter 6, provides a comprehensive summary of the ultimate experimental findings, results, and conclusions presented in the current thesis. Furthermore, it extends its purview to encompass an insightful exploration of the future trajectory of this work, addressing prospective areas of interest and potential avenues for continued research.

TABLE OF CONTENT

<i>Content</i>	<i>Pages</i>
<i>Chapter 1 Introduction</i>	<i>1</i>
1.1 Overview	1
1.2 VO ₂ : A Complex Mott Type Semiconductor.....	3
1.3 Significance of Resistive Switching.....	4
1.3.1 Hysteresis Width and Contrast	4
1.4 Literature Review.....	5
1.4.1 Magneli Phases of Vanadium Oxides	5
1.4.2 Vanadium Dioxide	6
1.4.3 Peierls Structural Transition	10
1.4.4 Mott Electronic Transition.....	12
1.4.5 Triggering the Phase Transition.....	12
1.4.6 Phase Stability	14
1.4.7 Semiconductor → Metal Transition Mechanism in VO ₂	15
1.4.8 Element Doping Effect in VO ₂	18
1.4.9 Application of VO ₂	20
1.5 Memristor and It's Characteristics.....	22
<i>REFERENCES</i>	<i>25</i>
<i>Chapter 2 Experimental Section: Materials Synthesis, Device Fabrication and Characterization Techniques</i>	<i>37</i>
2.1 Introduction.....	37
2.2 Sol-gel Method	40
2.3 Experimental Details.....	41
2.3.1 Materials.....	41
2.3.2 Synthesis of TiO ₂ Buffer Layer.....	41
2.3.3 Synthesis of Thin VO ₂ Films	42
2.3.4 Chemicals Bonding	43
2.3.5 Fabrication of TFMs.....	44
2.4 Material Characterization	46
2.4.1 X-ray Diffraction.....	47
2.4.2 Atomic Force Microscopy.....	49

2.4.3	<i>Field-Emission Scanning Electron Microscopy</i>	50
2.4.4	<i>High-Resolution Transmission Electron Microscopy</i>	51
2.4.5	<i>Raman Spectroscopy</i>	52
2.4.6	<i>Four-Probe Resistivity</i>	53
2.4.7	<i>X-ray Photoelectron Spectrophotometer</i>	54
2.4.8	<i>Scattering-Type Scanning Near-Field Optical Microscopy</i>	55
2.4.9	<i>Impedance Spectroscopy</i>	57
2.4.10	<i>Semiconductor Device Analyzer</i>	58
REFERENCES		59
Chapter 3 Observation of V-V Dimers Softening and Distinct Length Scales in Nanostructured VO₂ Thin Films.....		
		65
3.1	<i>Introduction</i>	65
3.2	<i>Results and Discussion</i>	67
3.2.1	<i>Structural Analysis with XRD</i>	67
3.2.2	<i>TEM Characterization</i>	68
3.2.3	<i>I-V Characteristics and Temperature Dependence of Sheet Resistance</i> ...	69
3.2.4	<i>Temperature Dependent Raman Spectroscopy</i>	71
3.2.5	<i>Numerical Simulation of Nucleation and Percolation Process During Phase Transition</i>	74
3.3	<i>Conclusion</i>	76
REFERENCES		78
Chapter 4 Charge Ordering at a Dielectric Gate in Itinerant Metallic States with Low-Field Memristor Properties in VO₂ Thin Film.....		
		81
4.1	<i>Introduction</i>	81
4.2	<i>Results and Discussion</i>	83
4.2.1	<i>Tailored Lattice Structure VO₂ at a Buffer Layer</i>	83
4.2.2	<i>XPS Bands in Charge Orders via Gate in VO₂ Films</i>	89
4.2.3	<i>I-V Characteristics in Field-Induced VO₂ Metallic States</i>	93
4.3	<i>Conclusion</i>	98
REFERENCES		99
Chapter 5 Successive VO₂ Phase Orders at Frequency Induced 3d^f Electrons Order of Metallizing Surface States in Thin VO₂@SiO₂-Si films.....		
		103
5.1	<i>Introduction</i>	103
5.2	<i>Results and Discussion</i>	104

5.2.1	<i>Thin Films VO₂@SiO₂-Si of Strained₀₁₁/_{d022} Layers</i>	104
5.2.2	<i>Dynamics of VO₂ Phase Order at Frequencies</i>	112
5.3	<i>Conclusion</i>	124
REFERENCES		126
Chapter 6 Conclusion and Future Plan		131
6.1	<i>Results and Conclusions</i>	131
6.2	<i>Future Scope of the Work</i>	133
Appendix:		
	<i>LIST OF PUBLICATIONS</i>	135
	<i>International Journals</i>	135
	<i>Comunicated Journals</i>	135
	<i>Conference Proceedings</i>	136
	<i>CONFERENCE/WORKSHOP/SEMINAR</i>	136
	<i>AWARD/ACHIEVEMENTS</i>	137
	<i>VITA</i>	139